Songklanakarin J. Sci. Technol.
40 (2), 430-438, Mar. - Apr. 2018

http://www.sjst.psu.ac.th

Original Article

Mechanical performance of consolidated crushed salt as backfill in boreholes and shafts

Supattra Khamrat and Kittitep Fuenkajorn*

Geomechanics Research Unit, Institute of Engineering,
Suranaree University of Technology, Mueang, Nakhon Ratchasima, 30000 Thailand

Received: 10 November 2016; Revised: 10 January 2017; Accepted: 16 January 2017

Abstract

Consolidation tests have been performed to determine the mechanical properties of crushed salt as affected by applied stresses and consolidation period. The crushed salt with particle sizes ranging from 0.075 to 4.76 mm mixed with 5% saturated brine are consolidated under axial stresses ranging from 2.5 to 10 MPa. The consolidation curves show instantaneous and transient creep strains. Densities, uniaxial compressive strengths and elastic moduli measured after consolidation for 3 to 180 days increase with the applied stresses and duration due to the particle rearrangement and recrystallization. The crushed salt properties are calculated as a function of mean strain energy required during consolidation. The opening depth and the time at which the crushed salt backfill is installed are significant factors controlling its long-term density, strength and stiffness.

Keywords: strain energy, consolidation, crushed salt, backfill, recrystallization

1. Introduction

Rock salt has become ones of the prominent ores associated with the Maha Sarakham formation in the northeast of Thailand. The excavations and penetrations of the formation can have a detrimental impact on the environment. Open shafts and boreholes may allow premature and unnecessary depressurization of the formation, and may result in wasting of natural resources. The sealing or backfilling can prevent or minimize the detrimental effects that may result from leaving the penetrations open. Salt mines have used the salt tailing as sealing material due to its availability, low cost and physical, chemical and mechanical compatibility with the host rock (Hansen, 1997; Holcomb & Hannum, 1982). The understanding of the consolidation behavior of crushed salt is thus the primary concern for the long-term assessment of the performance of the seal. The factors affecting the mechanical performance of consolidated crushed salt are moisture, duration, consolidation stresses, initial density, particle size and temperature (Pfeifle *et al.*, 1987; Shor *et al.*, 1981). The consolidation is effective only when moisture is available on grain contacts (IT Corporation, 1987; Wang *et al.*, 1992). As a consequence, dry crushed salt shows the lowest consolidation. Case *et al.* (1987) conclude from their experimental work that the volumetric creep strain rate increases with time and does not reach steady state values even after one to two months of load application. The uniaxial compressive strength and Young's modulus of crushed rock salt also increase with densification time (Miao *et al.*, 1995; Wang *et al.*, 1994).

A variety of constitutive models have been developed to predict the behavior of crushed salt consolidation in mine openings. They are derived from test results and can be presented in several forms of mathematical functions. Some that are notably mentioned include viscoelasticity (Munson & DeVries, 1991), elastic viscoplasticity (Van Sambeek, 1992), hot-pressing (Zeuch *et al.*, 1985), pressure solution (Spiers & Brzesowsky, 1993), healing mechanics (Miao *et al.*, 1995; Wang *et al.*, 1994) and empirical models (Sjaardema & Krieg, 1987). These models are complex and may not be suitable for the mining industry. They are specifically derived for the nuclear waste repository sealing. Most models are focused on the complex influence of temperature, moisture, density, creep and healing mechanisms on the properties of crushed salt under repository environ-

*Corresponding author
Email address: kittitep@sut.ac.th

ments. The results may be inappropriate for the relatively shallow salt mines where the closure rates of openings to be sealed are low (Hansen *et al.*, 1993). Even though the effects of consolidation on the physical and hydraulic behavior of crushed salt have been recognized and studied, experimental determination of the mechanical properties of crushed salt after consolidation has rarely been investigated. The long-term mechanical properties of the consolidated crushed salt after emplacement have never been assessed or predicted.

The objective of this study is to predict the mechanical properties of crushed salt backfill emplaced in boreholes and shafts. Consolidation tests are performed on crushed salt for the periods of 3 to 180 days. The mechanical properties of the specimens are determined as a function of the applied mean strain energy densities during consolidation. The time-dependent closure of borehole and shaft is calculated in terms of the released mean strain energy density. The crushed salt properties are predicted for different opening depths and installation periods.

2. Crushed Salt Sample

The crushed salt sample belongs to the Lower Member of the Maha Sarakham formation in the Khorat basin. Salt blocks are crushed by hammer mill to produce particle sizes ranging from 0.075 to 4.75 mm (Figure 1). The specific gravity is 2.160. This size range is equivalent to those expected to be obtained as waste product from the mines. The sphericity and roughness are determined from individual particles using an optical microscope. Based on the Power (1982) classification systems the crushed salt is classified as angular to sub-angular with spherical shape.

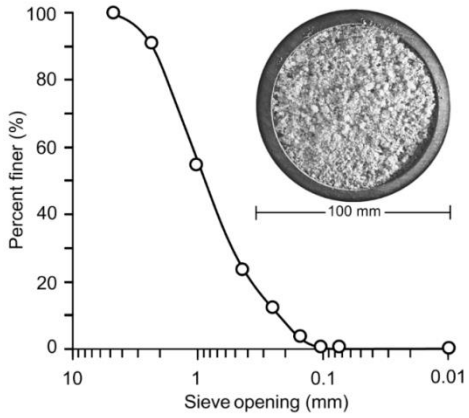

Figure 1. Grain size distribution of crushed salt.

Saturated brine is prepared by mixing rock salt with distilled water. The proportion of halite to water is about 39% by weight. Specific gravity of the saturated brine ($S.G._B$) is calculated as $S.G._B = \rho_{Brine}/\rho_{H_2O}$, where ρ_{Brine} is density of saturated brine (measured by a hydrometer in kg/m^3) and ρ_{H_2O} is density of water. The specific gravity of the saturated brine used here is 1.211 at 21°C.

3. Consolidation Test

3.1 Test apparatus and method

The consolidation tests are performed by applying constant axial stresses on the crushed salt mixed with saturated brine installed in a thick-wall stainless steel tube. The inner and outer diameters of the steel tube are 54 mm and 64 mm with the height of 200 mm (Figure 2a). Two loading pistons fitted with rubber O-rings are used to apply axial stress on the opposite ends of the specimen. The piston is 100 mm long with 53 mm in diameter. It has a drained hole to allow excess fluid to flow out during consolidation. A consolidation load frame applies constant stresses ranging from 2.5, 5, 7.5, to 10 MPa. The axial displacements are monitored by dial gages and are used to calculate the axial (consolidation) strains. The applied load is removed after 3, 5, 7, 10, 15, 30, 90, and 180 days. A total of 32 specimens have been tested.

The suitable brine content is first determined by applying consolidation stresses from 2.5, 5.0, 7.5 to 10 MPa to the crushed salt mixed with saturated brine from 0%, 5% to 10% by weight. The crushed salt and brine are mixed thoroughly in a plastic pan until each salt particle is coated with thin film of brine. This process takes about 5 minutes. The mixture is then poured into the steel tube and lightly tapped to obtain a flat end. The initial length of specimen is obtained as 140 mm before inserting the loading pistons. This is equivalent to the initial volume of 316.8 cm^3. This results in the initial densities before loading of 1.184, 1.247 and 1.310 g/cm^3 for the 0%, 5% and 10% brine contents. The results indicate that axial strain increases with the brine content (Figure 2b). The dry crushed salt has the lowest consolidation. This agrees with results obtained by Shor *et al.* (1981) and Wang *et al.* (1992) that a small amount of fluid can significantly enhance the consolidation rate. The axial strains obtained at 5% and 10% brine contents are similar. The saturated brine content used in this study is therefore maintained constant at 5% by weight with the constant initial density of 1.247 g/cm^3. This initial density is maintained constant for all test samples by controlling the constant initial sample volume at 316.8 cm^3 (length = 140 mm and diameter = 54 mm).

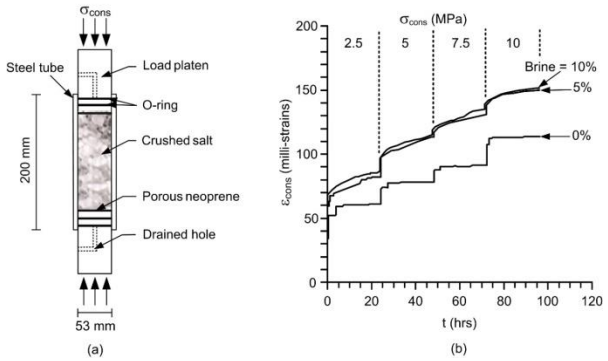

Figure 2. Consolidation steel tube (a) and axial strains as a function of time for different axial stresses and brine contents (b).

3.2 Consolidation test results

Figure 3 shows the axial strains (ε_{cons}) as a function of consolidation period (t) up to 180 days. A higher applied consolidation stress (σ_{cons}) leads to a larger strain. The strains increase immediately after the axial stress is applied. The strain rates decrease with time, and tend to remain relatively unchanged after 30 days. The samples under the same applied stress show the same trend of the ε_{cons}–t curves, suggesting that the test results are repeatable and the consolidation procedure is reliable.

The deformation of the crushed salt may be divided into two phases: instantaneous and transient deformations. The mechanism governing the instantaneous deformation is the rearrangement of the salt particles which occurs immediately after load application (Callahan *et al.*, 1996; Hwang *et al.*, 1993). The transient phase involves cracking and sliding between salt particles and creep deformation of the salt particles. This leads to the deceleration of the deformation.

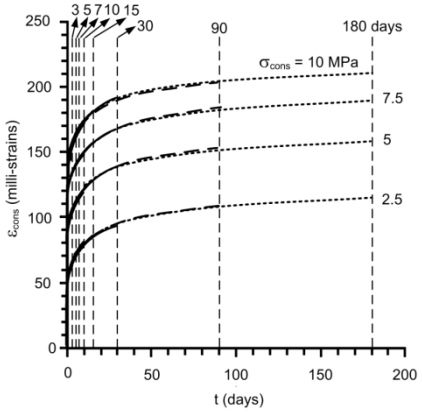

Figure 3. Axial strain (ε_{cons}) as a function of consolidation period (t) for different consolidation stresses (σ_{cons}). Vertical dash lines indicated the time at which each specimen is removed from the steel tube.

4. Mechanical Properties of Consolidated Crushed Salt

To assess the mechanical properties of the consolidated crushed salt the specimens are removed from the steel tube after 3, 5, 7, 10, 15, 30, 90, and 180 days. They appear solidified, particularly under long consolidation period and high stress. The specimen ends are dried-cut to obtain flat and parallel surfaces. The length-to-diameter ratios are about 2.0-2.2. The specimen density after removed from the steel tube is measured. A higher applied consolidation stress leads to a higher density (Table 1). The density increases rapidly from 1.247 g/cm^3 within three days after load application. The increasing rate reduces after 15 days of consolidation. The specimen compressive strengths and elastic parameters are determined in accordance with the ASTM (D2938-95) (ASTM International, 2002). standard practice. Figure 4 shows the stress-strain curves obtained from different consolidation stresses and periods. Larger consolidation period and stress lead to higher strength and elasticity of the specimens (Figure 5b and c). This effect becomes larger under higher σ_{cons}. The Poisson's ratios however decrease slightly with increasing consolidation period (Figure 5d). The results suggest that the crushed salt becomes denser, stiffer, stronger and less compressible with time and applied stress. This generally agrees with the results obtained from Wang *et al.* (1994) and Miao *et al.* (1995) who performed uniaxial compression test on compacted crushed salt specimens. They report that under 15 MPa consolidation stresses the strength and elastic modulus increase up to 28.4 MPa and 9.46 GPa after being consolidated for 97 days.

Table 1. Mechanical properties of crushed salt after consolidation.

σ_{cons} (MPa)	Parameters	t (days)							
		3	5	7	10	15	30	90	180
2.5	ρ (g/cm^3)	1.34	1.35	1.35	1.36	1.37	1.38	1.41	1.42
	σ_c (MPa)	N/A	0.52	1.03	1.22	1.62	1.98	3.23	5.10
	E (MPa)	N/A	62.0	74.1	82.0	100.3	110.9	139.9	160.0
	ν	N/A	0.38	0.37	0.37	0.37	0.36	0.35	0.34
5	ρ (g/cm^3)	1.41	1.42	1.42	1.43	1.44	1.46	1.48	1.49
	σ_c (MPa)	2.01	2.03	2.60	3.34	4.14	4.82	7.38	10.51
	E (MPa)	121.0	142.2	160.2	172.2	180.1	199.9	230.2	280.1
	ν	0.36	0.35	0.35	0.35	0.34	0.33	0.32	0.31
7.5	ρ (g/cm^3)	1.45	1.46	1.47	1.48	1.49	1.51	1.54	1.55
	σ_c (MPa)	3.78	4.15	4.82	5.50	6.48	7.28	11.71	15.06
	E (MPa)	189.3	213.2	229.4	250.0	260.0	291.0	331.9	400.1
	ν	0.34	0.34	0.33	0.33	0.32	0.31	0.30	0.30
10	ρ (g/cm^3)	1.50	1.50	1.51	1.53	1.54	1.56	1.58	1.58
	σ_c (MPa)	6.20	6.52	7.10	7.51	8.21	10.00	15.07	19.02
	E (MPa)	271.0	299.9	321.0	340.9	361.2	370.1	438.9	500.0
	ν	0.31	0.31	0.30	0.30	0.30	0.29	0.29	0.28

Notes: The initial density for all samples is controlled constant at 1.247 g/cm^3.

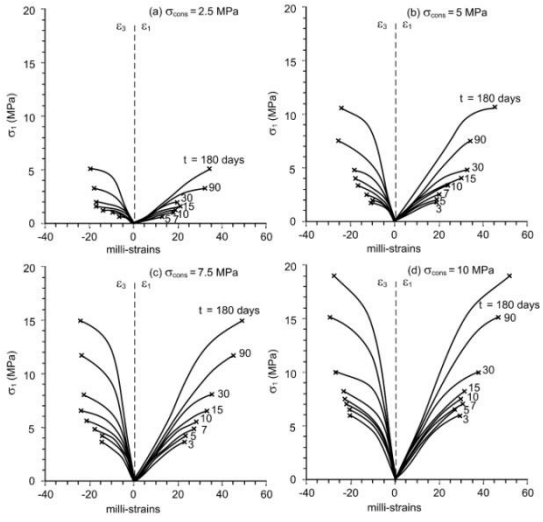

Figure 4. Stress-strain curves obtained from uniaxial compressive strength testing of crushed salt specimens after consolidation.

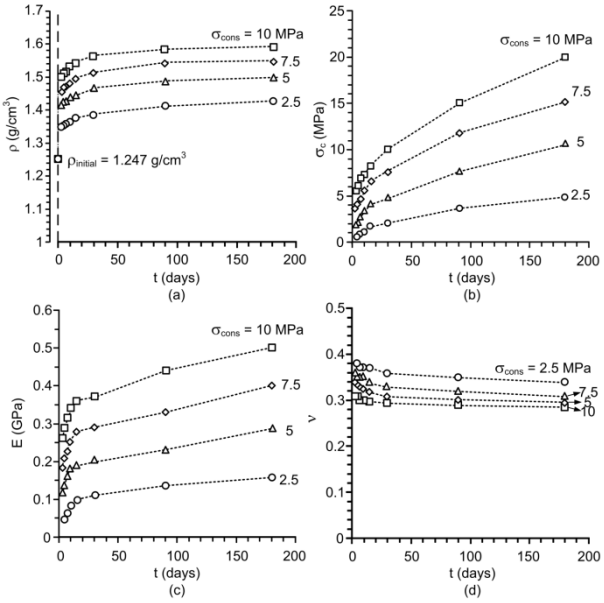

Figure 5. Density (a), uniaxial compressive strength (b), elastic modulus (c) and Poisson's ratio (d) as a function of consolidation period (t) for different consolidation stresses (σ_{cons}).

5. Strain Energy Density Principle

The strain energy density principle is applied here to determine the energy required to consolidate the crushed salt under different stresses and periods. It is postulated that the crushed salt can be consolidated by applying the mean strain energy (W_m). This energy can be calculated from mean stresses (σ_m) and strains (ε_m) (Jaeger *et al.*, 2007):

$$W_m = (3/2) \cdot \sigma_m \cdot \varepsilon_m \quad (1)$$

$$\sigma_m = (\sigma_1+\sigma_2+\sigma_3)/3 \quad (2)$$

$$\varepsilon_m = (\varepsilon_1+\varepsilon_2+\varepsilon_3)/3 \quad (3)$$

The lateral stresses (σ_2 and σ_3) on the specimen can be calculated as a function of time based on the uniaxial strain condition, i.e. assuming that no lateral strain occurs in the steel tube during consolidation. The axial strains from the measurement results therefore represent the volumetric strain.

$$\sigma_2 = \sigma_3 = [\nu / (1-\nu)] \sigma_1 \quad (4)$$

where ν is Poisson's ratio, and σ_1 is consolidation stress (σ_{cons}). The calculated mean stress, strain and strain energy density are given in Table 2.The specimens under higher consolidation stress and time lead to higher mean strain energy densities.

6. Crushed Salt Properties as a Function of Mean Strain Energy Density

An attempt is made to correlate the crushed salt properties with the applied mean strain energy density during consolidation. It is first postulated that two main mechanisms govern the changes of the properties of crushed salt: consolidation and recrystallization (Callahan *et al.*,1996). The first mechanism involves the volumetric reduction of the crushed salt mass by particle rearrangement, creep, cracking and sliding between grain boundaries. It is reflected by instantaneous and transient deformations which are mainly controlled by the applied energy. The second mechanism involves the recrystallization and healing between salt particles (Hansen, 1997; Hwang *et al.*, 1993). This mechanism does not decrease the crushed salt volume. It can however strengthen and stiffen the specimen as the consolidation period increases.

Table 2. Mean stresses and strains and mean strain energy densities applied to crushed salt during consolidation.

σ_{cons} (MPa)	Parameters	t (days)							
		3	5	7	10	15	30	90	180
2.5	σ_m (MPa)	N/A	1.85	1.81	1.81	1.81	1.77	1.73	1.69
	ε_m (10^{-3})	N/A	23.33	25.00	26.67	29.33	31.67	35.00	38.33
	W_m(MPa)	N/A	0.058	0.062	0.066	0.073	0.079	0.067	0.095
5	σ_m (MPa)	3.54	3.46	3.46	3.46	3.38	3.31	3.24	3.16
	ε_m (10^{-3})	33.33	38.00	39.33	40.33	42.67	46.00	50.00	56.67
	W_m(MPa)	0.165	0.188	0.195	0.200	0.212	0.228	0.248	0.281
7.5	σ_m (MPa)	5.03	4.97	4.96	4.90	4.85	4.75	4.64	4.63
	ε_m (10^{-3})	41.67	47.33	49.00	50.33	53.33	56.00	61.33	66.67
	W_m(MPa)	0.310	0.352	0.365	0.374	0.397	0.417	0.456	0.496
10	σ_m (MPa)	6.33	6.33	6.19	6.19	6.19	6.12	6.06	5.99
	ε_m (10^{-3})	53.33	55.67	57.33	58.33	61.33	63.33	67.67	70.00
	W_m(MPa)	0.530	0.553	0.569	0.579	0.609	0.629	0.672	0.695

6.1 Crushed salt density

Based on the concept above the change of the crushed salt density (ρ) can be represented by:

$$\rho = \rho_{initial} + \Delta\rho_{cons} \quad (5)$$

where $\rho_{initial}$ is the initial density before applying the mean strain energy (equal to 1.247 g/cm^3)and $\Delta\rho_{cons}$ is the reduction of bulk density due to the strain energy and consolidation period. Regression analysis of the test data (Figure 5) by SPSS software (Wendai, 2000) can determine $\Delta\rho_{cons}$ as a function of W_m and t:

$$\Delta\rho_{cons} = 0.044 \cdot W_m^{0.391} \cdot t^{0.059} (g/cm^3) \quad (6)$$

Good correlation is obtained (R^2>0.9). Figure 6a compares the curve fits with the test results. It should be noted that the crushed salt density is independent of the recrystallization and healing because these processes do not reduce the bulk volume of specimens.

6.2 Crushed salt porosity

Similar to the density prediction above the reduction of crushed salt porosity (n) during consolidation can be determined by the regression analysis of the test data:

$$n = n_{initial} - \Delta n_{cons} \quad (7)$$

where $n_{initial}$ is the initial crushed salt porosity (42%) and Δn_{cons} is the porosity reduction which can be represented by a power equation:

$$\Delta n_{cons} = 480.203 \cdot W_m^{0.411} \cdot t^{0.070} \quad (\%) \quad (8)$$

The diagrams in Figure 6b suggest that the applied mean strain energy affects the porosity reduction and the density increase more than does the consolidation period.

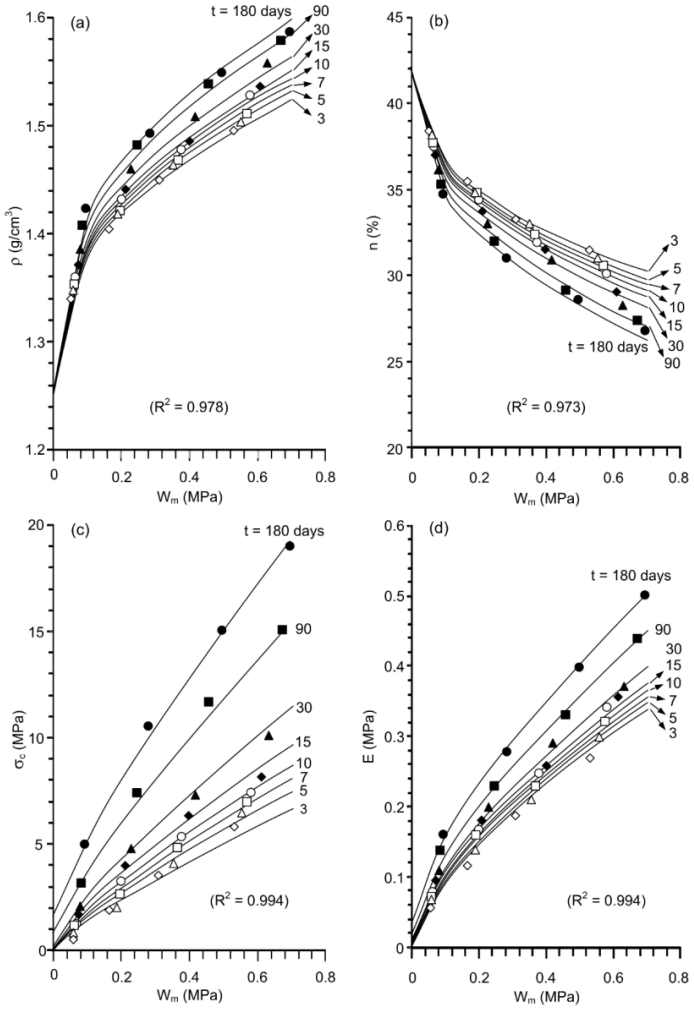

Figure 6. Density (a), porosity (b), uniaxial compressive strength (c) and elastic modulus (d) as a function of mean strain energy density (W_m).

6.3 Crushed salt strength

The crushed salt strength (σ_c) is controlled by both consolidation and recrystallization. The effects from the two mechanisms can be superimposed as:

$$\sigma_c = \Delta\sigma_{c,cons} + \Delta\sigma_{c,rec} \quad (9)$$

where $\Delta\sigma_{c,cons}$ is the strength increase due to consolidation and $\Delta\sigma_{c,rec}$ is the strength increase by recrystallization. They can be represented by the following empirical equations:

$$\Delta\sigma_{c,cons} = 6.873 \cdot W_m^{0.799} \cdot t^{0.220} \quad \text{(MPa)} \quad (10)$$

$$\Delta\sigma_{c,rec} = 0.009 \cdot t \cdot \exp(W_m) \text{(MPa)} \quad (11)$$

The empirical constants are obtained from the regression analysis of the test data using equation (9). Figure 6c compares the predictions with the test results. Note that under $W_m = 0$ the specimen strength can increase with time due to the recrystallization and healing.

6.4 Crushed salt elastic modulus

The crushed salt elastic modulus (E) is also controlled by both consolidation and recrystallization mechanisms:

$$E = \Delta E_{cons} + \Delta E_{rec} \quad (12)$$

where ΔE_{cons} is the increase of elastic modulus due to consolidation and ΔE_{rec} is the increase of elastic modulus by recrystallization. They can be represented by:

$$\Delta E_{cons} = 0.399 \cdot W_m^{0.658} \cdot t^{0.061} \quad \text{(MPa)} \quad (13)$$

$$\Delta E_{rec} = 0.0002 \cdot t \cdot \exp(W_m) \quad \text{(MPa)} \quad (14)$$

The empirical constants are obtained from the regression analysis using equation (12). Figure 6d shows that the elasticity of crushed salt can increase with time even without the applied mean strain energy ($W_m = 0$).

7. Circular Opening in Salt Mass Subjected to Uniform External Pressure

The mean strain energy released by creep closure of circular openings (shaft or borehole) in infinite salt mass subjected to uniform external pressure (in-situ stress) is determined and used to predict the changes of the crushed salt properties after emplacement. The released energy ($W_{m,s}$) can be calculated from the stresses and strains at the opening wall as:

$$W_{m,s} = (3/2) \cdot [(\sigma_r + \sigma_\theta + \sigma_z)/3] \cdot [(\varepsilon_r + \varepsilon_\theta + \varepsilon_z)/3] \quad (15)$$

where σ_r, σ_θ and σ_z are radial, tangential and axial stresses and ε_r, ε_θ and ε_z are radial, tangential and axial strains.

Under plane strain condition the radial and tangential stresses obtained from the Kirsch's solution can be presented as (Jaeger *et al.*, 2007):

$$\sigma_r = [1 - (a^2/r^2)] \cdot P_o \quad (16)$$

$$\sigma_\theta = [1 + (a^2/r^2)] \cdot P_o \quad (17)$$

where P_o is external pressure, a is opening radius and r is radial distance from the center. The axial stress (σ_z) can be determined by:

$$\sigma_z = \nu(\sigma_r + \sigma_\theta) \quad (18)$$

At the opening boundary the strains are defined as:

$$\varepsilon_r = \varepsilon_r^e + \varepsilon_r^c \quad (19)$$

$$\varepsilon_z = \varepsilon_\theta = 0 \quad (20)$$

where ε_r^e is the elastic radial strain and ε_r^c is the time-dependent radial strain controlling the creep closure of the opening.

The elastic radial strain can be obtained by (Jaeger *et al.*, 2007):

$$\varepsilon_r^e = \frac{1}{E}\left\{(1-\nu^2)\sigma_r - \nu(1+\nu)\sigma_\theta\right\} \quad (21)$$

Nair and Boresi (1970) and Fuenkajorn and Daemen (1988) have derived the radial creep strain around circular hole based on the potential creep law and the associated flow rule as:

$$\varepsilon_r^c = \frac{3}{2}\kappa(\sigma^*)^{(\beta-1)} \cdot S_r\left(t_1^\gamma - t_0^\gamma\right) \quad (22)$$

where κ, β and γ are material constants of the potential creep law, S_r is the radial stress deviation, and σ^* is the equivalent (effective) stress. The stress deviation can be obtained from:

$$S_r = \sigma_r - (\sigma_r + \sigma_\theta + \sigma_z)/3 \quad (23)$$

Based on the von Mises flow rule σ^* is defined as:

$$\sigma^* = \frac{1}{\sqrt{2}}\left\{(\sigma_r - \sigma_\theta)^2 + (\sigma_\theta - \sigma_z)^2 + (\sigma_z - \sigma_r)^2\right\}^{\frac{1}{2}} \quad (24)$$

Substituting equations (16) to (24) into equation (15) the released mean strain energy (by closure) at the opening boundary can be calculated.

To demonstrate the application of the strain energy concept used here, the mechanical and rheological parameters of the Maha Sarakham salt obtained from Wilalak and Fuenkajorn (2016) are assigned to the equations above, where $\kappa = 0.0003$ 1/MPa·day, $\beta = 1.43$ and $\gamma = 0.218$. The elastic parameters are obtained from Luangthip *et al.* (2016) who report the elastic modulus = 16.89 GPa and Poisson's ratio = 0.27 for the Lower Member of the Maha Sarakham formation. The released energy at the opening boundary is calculated for the external pressures of 5, 10 and 15 MPa (equivalent to the depths approximately of 200, 370 and 550 m). Figure 7a plots the released strain energy density ($W_{m,s}$) as a function of time after excavation. The $W_{m,s}$ increases rapidly after excavation particularly during the first year. The rate of releasing energy

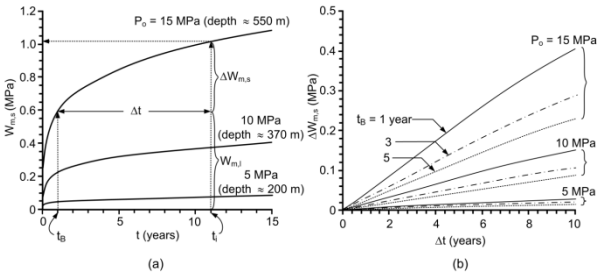

Figure 7. Mean strain energy density ($W_{m,s}$) released from closure of circular openings under different P_o's (a) and remaining mean strain energy density ($\Delta W_{m,s}$) as a function of time after backfill emplacement (b).

reduces with time. The greater external pressures (deeper opening) lead to the larger released energy. The diagrams suggest that the time at which the crushed salt backfill is installed (t_B) is a significant factor dictating the amount of released energy remaining for consolidating the crushed salt backfill.

8. Prediction of Crushed Salt Properties after Emplacement

To predict the crushed salt properties after emplacement, the strain energy left for the consolidation is needed. It can be obtained from:

$$\Delta W_{m,s} = W_{m,s} - W_{m,l} \quad (25)$$

where $W_{m,s}$ is the total released energy from excavation to any selected period (t_i) determined as if no backfill is installed, and $W_{m,l}$is the energy lost due to creep closure before backfill is installed. The time at which the backfill is installed is designated as t_B in Figure 7a. The duration for consolidation (Δt) can be obtained from:

$$\Delta t = t_i - t_B \quad (26)$$

The $\Delta W_{m,s}$ at depths of 200, 370 and 550 m are calculated for t_B = 1, 3, and 5 years. The prediction period (Δt) is up to 10 years after emplacement. From equation (25) $\Delta W_{m,s}$can be calculated as a function of Δt as shown in Figure 7b. The results indicate that the $\Delta W_{m,s}$values increase with time (Δt). This is due to the fact that the released energy by creep closure of the opening after backfill emplacement is contributed by the increase of the radial stresses and the decrease of the radial strain rate at the opening boundary. This is caused by the mechanical interaction between the opening wall and the installed crushed salt. The effect of $t_B$is more pronounced under high P_o than under low P_o. This implies that the time at which the crushed salt backfill is installed is more critical for deep openings than for the shallow ones.

Substituting $\Delta W_{m,s}$and Δt values from Figure 7b into W_m and t values in Equations (5) through (14) the density, porosity, compressive strength and elastic modulus can be predicted, as shown in Figure 8. For this demonstration the predictions are made up to 10 years. The results suggest that the crushed salt density increases with time (Δt) from its

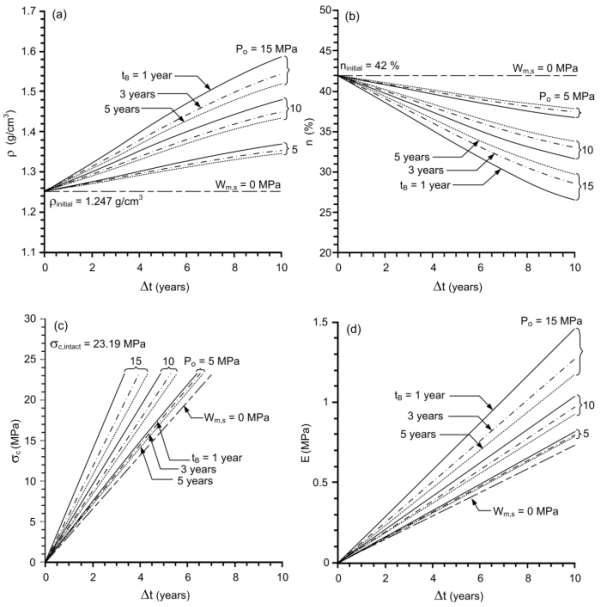

Figure 8. Density (a), porosity (b), uniaxial compressive strength (c) and elastic modulus (d) of crushed salt as a function of time after emplacement in circular opening.

initial value of 1.247 g/cm^3 (Figure 8a). Subsequently the corresponding porosity decreases with Δt (Figure 8b). Without applying W_m the density and porosity of the crushed salt backfill remain unchanged. Both σ_c and E increase with P_o and Δt (Figure 8c, d). Under no W_m application they can also increase with time due to the recrystallization and healing. The effects of t_B on the strength and elasticity are more pronounced for the crushed salt backfill installed in deep openings than in shallow openings.

9. Conclusions and Discussion

A total of 32 crushed salt specimens have been consolidated under periods of 3 to 180 days. These are the longest consolidation periods as compared to the experimental work performed elsewhere on crushed salt. The results are believed to be reliable as evidenced by the overlapping (repeating) of the measured axial strains under different periods with the same σ_{cons}. Effort has been made here to obtain the density, strength and elastic parameters of the crushed salt after being consolidated under various stresses and durations (Table 1). The results lead to the development of the empirical formulae relating the crushed salt properties with the applied mean strain energy density. The application of the strain energy principle allows considering both stress and strain to which the crushed salt specimens are subjected (Figure 6). This approach is considered more fundamental and simpler than those of the complex creep and healing constitutive equations proposed elsewhere for the sealing of nuclear waste repository.

Two main mechanisms simultaneously occur in the crushed salt: (1) consolidation by volumetric change due to particle rearrangement and cracking and creep of the salt crystals, and (2) recrystallization and healing processes. Both can strengthen and stiffen the crushed salt mass.

The prediction of the crushed salt properties after emplacement in shaft and borehole presented here may be conservative because the axial load imposed by the backfill gravity is excluded from the calculation. Depending on the emplacement depth the weight of the crushed salt backfill can contribute to the mean strain energy applied to the crushed salt.

It is clear from the findings obtained here that the time at which the backfill is installed (t_B) is an important factor to increase the mechanical performance of the crushed salt, particularly under great depth. Under shallow depth the crushed salt density and porosity cannot be effectively increased because the available mean strain energy at the opening boundary is low. The strength and elastic parameters can nevertheless be improved even under shallow depth (low mean strain energy). This is because these mechanical properties are governed by both consolidation and recrystallization.

The diagrams in Figure 8 can be used as a guideline for the backfill planning and for the performance assessment of the crushed salt backfill properties. Care should be taken to apply the results obtained here to other salt formations and locations. Different grain size distributions and moisture contents of the crushed salt are likely to result in different consolidation behaviors. The mechanical properties predictions are also sensitive to the creep parameters calibrated from the laboratory test results. Application of different constitutive creep models for the surrounding salt mass may also result in different predictions of the crushed salt properties.

Acknowledgements

This study is funded by Suranaree University of Technology and by the Higher Education Promotion and National Research University of Thailand. Permission to publish this paper is gratefully acknowledged.

References

ASTM International. (2002). *Standard test method for unconfined compressive strength of intact rock core specimens* (ASTM D2938-95). Retrieved from https://www.astm.org/Standards/D2938

Callahan, G. D., Loken, M. C., Hurtads, L. D., & Hansen, F. D. (1996). Evaluation of constitutive models for crushed salt. *Proceedings of the 5th Mechanical Behavior of Salt 1996*, 317-330.

Case, J. B., Kelsall, P. C., & Withiam, J. L. (1987). Laboratory investigation of crushed salt consolidation. *Proceedings of the 28th U.S. Symposium on Rock Mechanics (USRMS)*, Tucson, AZ.

Fuenkajorn, K., & Daemen, J. J. K. (1988). *Borehole closure in salt*. Tucson, AZ: University of Arizona.

Hansen, F. D. (1997). Reconsolidating salt: Compaction, constitutive modeling, and physical processes. *International Journal of Rock Mechanics and Mining Sciences, 34*(3–4), 119.e1–119.e12.

Hansen, F. D., Callahan, G. D., & Van Sambeek, L. L. (1993). Reconsolidation of salt as applied to permanent seals for the waste isolation pilot plant. *Proceedings of the 3rd on the Mechanical Behavior of Salt 1993*, 323-335.

Holcomb, D. J., & Hannum, D. W. (1982). *Consolidation of crushed-salt backfill under conditions appropriate to the WIPP facility* (Report No. SAND82-0630). Retrieved from https://inis.iaea.org/search/search.aspx?orig_q=RN:14756354

Hwang, C. L., Wang, M. L., & Miao, S. (1993). Proposed healing and consolidation mechanisms of rock salt revealed by ESEM. *Microscopy Research and Technique, 25*(5–6), 456-464.

IT Corporation. (1987). *Laboratory investigation of crushed salt consolidation and fracture healing* (Report No. BMI/ONWI-631). Retrieved from https://www.osti.gov/servlets/purl/6839572

Jaeger, J. C., Cook, N. G. W., & Zimmerman, R. W. (2007). *Fundamentals of Rock Mechanics* (4thed.). Victoria, Australia: Blackwell Publishing.

Luangthip, A., Khamrat, S., & Fuenkajorn, K. (2016). Effects of carnallite contents on stability and extraction ratio of potash mine. *Proceedings of the 9th Asian Rock Mechanics Symposium*, Bali, Indonesia.

Miao, S., Wang, M. L., & Schreyer, H. L. (1995). Constitutive models for healing of materials with application to compaction of crushed rock salt. *Journal of Engineering Mechanics, 121*(10), 1122-1129.

Munson, D., & Devries, K. (1991). Development and validation of a predictive technology for creep closure of underground rooms in salt. *Proceedings of the 7th ISRM Congress*, Aachen, Germany.

Nair, K., & Boresi, A. P. (1970). Stress analysis for time dependent problems in rock mechanics. *Proceedings of the 2nd Congress of the International Society for Rock Mechanics: Belgrade 2*(4), 531-536.

Pfeifle, T. W., Senseny, P. E., & Mellegard, K. D. (1987). *Influence of variables on the consolidation and unconfined compressive strength of crushed salt, technical report* (Report No. BMI/ONWI-627). Retrieved from https://inis.iaea.org/search/search.aspx?orig_q=RN:18066253

Power, M. C. (1982). Comparison charts for estimating roughness and shericity, AGI data sheets. Alexandria, VA: American Geological Science Institute.

Shor, A. J., Baes, C. F., & Canonico, C. M. (1981). *Consolidation and permeability of salt in Brine* (Report No. ORNL-5774). Retrieved from https://www.osti.gov/servlets/purl/6209215

Sjaardema, G. D., & Krieg, R. D. (1987). *A constitutive model for the consolidation of WIPP crushed salt and its use in analyses of backfilled shaft and drift configurations* (Report No. SAND87-1977). Retrieved from https://www.osti.gov/biblio/5752133

Spiers, C. J., & Brzezowski, R. H. (1993). Densification behavior of wet granular salt: Theory versus experimental. *Proceedings of the 7th Symposium on Salt, Amsterdam 1993*, 83-92.

Van Sambeek, L. L. (1992). Testing and modelling of backfill used in salt and potash mines. *Proceedings of the Rock Support in Mining and Underground Construction, Balkema, Rotterdam 1992*, 583-589.

Wang, M. L., Maji, A. K., & Miao, S. (1994). Deformation mechanisms of WIPP backfill. *Radioactive Waste Management and the Nuclear Fuel Cycle*, 20(2-3), 191-211.

Wang, M. L., Miao, S. K., Maji, A. K., & Hwang, C. L. (1992). Effect of water on the consolidation of crushed rock salt. *Proceedings of the Engineering Mechanics, ASCE 1992*, 531-534.

Wendai, L. (2000). *Regression analysis, linear regression and profit regression.* Beijing, China: Publishing House of Electronics Industry.

Wilalak, N., & Fuenkajorn, K. (2016). Constitutive equation for creep closure of shaft and borehole in potash layers with varying carnallite contents. *Proceedings of the 9th Asian Rock Mechanics Symposium*, Bali, Indonesia.

Zeuch, D. H., Holcomb, D. J., & Lauson, H. S. (1985). *Analysis of consolidation of granulated rocksalt using a plastic flow model of isostatic hot-pressing* (Report No. SAND84-1106). Retrieved from https://www.osti.gov/biblio/6123970-analysis-consolidation-granulated-rocksalt-using-plastic-flow-model-isostatic-hot-pressing